

**NASA Technical Memorandum 86231**

**Excitation of the Earth's  
Chandler Wobble by Southern  
Oscillation / El Nino,  
1900-1979**

{NASA-TM-86231} EXCITATION OF THE EARTH'S  
CHANDLER WOBBLE BY SOUTHERN OSCILLATION/EL  
NINO, 1900-1979 (NASA) 23 p HC A02/MF A01  
CSCL 08E

N86-19713

Unclas  
03934

G3/43

**B. Fong Chao**

September 1985

**NASA**



**NASA Technical Memorandum 86231**

**Excitation of the Earth's  
Chandler Wobble by Southern  
Oscillation / El Nino,  
1900-1979**

**B. Fong Chao**  
*Geodynamics Branch*  
*Laboratory For Terrestrial Physics*  
*Goddard Space Flight Center*  
*Greenbelt, Maryland 20771*

**September 1985**

**NASA**

National Aeronautics and  
Space Administration

**Goddard Space Flight Center**  
Greenbelt, Maryland 20771

**1985**

**Page intentionally left blank**

**Page intentionally left blank**

EXCITATION OF THE EARTH'S CHANDLER WOBBLE  
BY SOUTHERN OSCILLATION / EL NINO, 1900-1979

ABSTRACT

The southern oscillation / El Nino (ENSO) is the single most prominent interannual signal in global atmospheric/oceanic fluctuations. This paper addresses the following question: how important is the angular momentum carried by ENSO in exciting the Earth's Chandler wobble? The question is attacked through a statistical analysis of the coherence spectra (correlation as a function of frequency) between two data sets spanning 1900-1979—the southern oscillation index (SOI) time series and the excitation function  $\psi$  (with x-component  $\psi_x$  and y-component  $\psi_y$ ) of the Chandler wobble derived from the homogeneous ILS (International Latitude Service) polar motion data. The coherence power and phase in the Chandler frequency band ( $\sim 0.79$ – $0.89$  cpy) are studied. It is found that, during 1900-1979 the coherence between SOI and  $\psi_x$  is significant well over the 95% confidence threshold whereas that between SOI and  $\psi_y$  is practically nil. Quantitatively, the coherence study shows that ENSO provides some 20% of the observed Chandler wobble excitation power. Since earlier investigations have shown that the total atmospheric/oceanic variation can account for the Chandler wobble excitation at about 20% level, the implication is that ENSO may be an important (interannual) part of the atmospheric/oceanic variation that is responsible for the Chandler wobble excitation during 1900-1979.

PRECEDING PAGE BLANK NOT FILMED

EXCITATION OF THE EARTH'S CHANDLER WOBBLE  
BY SOUTHERN OSCILLATION / EL NINO, 1900-1979

1. INTRODUCTION

The southern oscillation (SO) is the single most prominent signal in interannual, global-scale atmospheric fluctuations. It is characterized by an irregular seesawing of air mass between the Eastern and Western Hemispheres in the tropical Pacific-Indian Ocean region. For some as yet unknown reasons, every once in a few years the SO wind field will collapse and, through ocean-atmosphere interactions, cause extensive meteorological disruptions—a phenomenon known as an El Nino event. In keeping with meteorological terminology, the whole southern oscillation / El Nino system will be referred to as ENSO.

The Earth's rotation axis does not remain fixed relative to the body of the Earth. Instead, it traces out on the surface of the Earth a quasi-periodic path about some slowly drifting mean position near the Poles. This motion is known as the polar motion. The Chandler wobble is a major component in the polar motion. It is a free oscillation of the Earth (corresponding to the Eulerian free nutation) and has a period of about 14 months. From decades of observation we know that the Chandler wobble has been continually excited. The major mechanism of excitation, however, is presently unknown despite a great deal of effort by many investigators over the years.

The present paper studies the importance of the great amount of atmospheric angular momentum carried by ENSO in the excitation of the Chandler wobble. Through the conservation of angular momentum, any atmospheric angular momentum change is coupled to the rotation of the solid Earth, resulting in changes in length-of-day and polar motion. In fact, the atmospheric angular momentum associated with ENSO has been shown to have a major influence on the interannual length-of-day variations over the last 3 decades since accurate measurements were available (Chao, 1984), the most dramatic example being the extraordinarily strong 1982-1983

ENSO event (see also Rosen et al., 1984; Eubanks et al., 1985). As for polar motion, the latter event has been demonstrated by Gross & Chao (1985) to have a good temporal correlation with the y-component of the excitation function of the Chandler wobble, suggesting that this event is also a major excitation mechanism for the Chandler wobble during 1982-1983. Now the question arises: what about earlier El Nino events? More precisely, how important, as far as we can tell from available data, is ENSO in the excitation of Chandler wobble?

The nature of the question suggests a statistical correlation study. Following Munk & Hassan (1961) and Wilson & Haubrich (1976), this paper studies the correlation in the frequency domain (i.e. the coherence spectra) and concentrate only on the Chandler band which can be loosely defined as the frequency band centered at 0.84 cycles per year (cpy), corresponding to a period of about 14 months, with a bandwidth of about 0.1 cpy. This is because the Chandler band is where the excitation energy of the Chandler wobble resides. It, along with the annual frequency band, is also where the polar motion observations have the highest signal-to-noise ratio. If any correlation between ENSO and Chandler wobble exists, it should show up in the coherence spectra within the Chandler band.

In order to secure statistical stability and, at the same time, achieve reasonable frequency resolution, we need data records as long as we can get. This paper uses polar motion and SO time series spanning the period 1900-1979. They are described in the next section.

## 2. DATA PREPARATION

The strength of SO is customarily measured by the (dimensionless) SO Index (SOI), defined as

$$\text{SOI}(\text{Yr}, \text{Mo}) = [\text{SLP}(\text{Yr}, \text{Mo})]_{\text{Tahiti}} - [\text{SLP}(\text{Yr}, \text{Mo})]_{\text{Darwin}} \quad (1)$$

where  $\text{SOI}(\text{Yr}, \text{Mo})$  is the SOI at month  $\text{Mo}$  of year  $\text{Yr}$ ; and  $\text{SLP}(\text{Yr}, \text{Mo})$  is the atmospheric pressure at sea level normalized by its standard deviation for month  $\text{Mo}$  obtained from many decades of observation at a given station, after removal of the corresponding mean value for month  $\text{Mo}$ . The SOI thus defined is a zero-mean, monthly time series devoid of seasonal and geographical effects at the two stations which represent the eastern and western centers of the (seasawing) SO system. The observation of SLP at Darwin has been available since 1882, but did not start at Tahiti until 1935. Fortunately, the SLP (especially the low-frequency variations therein) at Tahiti and at Darwin are highly correlated—they are virtually mirror images of each other (see, e.g., Rasmusson & Wallace, 1983). Therefore, I simply substitute into Equation (1) the relation  $(\text{SLP})_{\text{Tahiti}} = -(\text{SLP})_{\text{Darwin}}$  to obtain pre-1935 SOI values. I then pass the entire 1900–1979 SOI time series thus constructed through a moderate low-pass filter with corner frequency at 2.5 cpy. The result is presented as Figure 1(c). During this period there are some 30 El Niño events (see, e.g., Quinn et al., 1978). Although not indicated in the Figure, they are in general associated with pronounced drops in the SOI value.

The polar motion data set used is the homogeneous ILS (International Latitude Service) data set reduced by Yumi & Yokoyama (1980). It consists of two monthly time series: the x-component along the Greenwich meridian and the y-component along the 90°E longitude. Spanning 80 years from 1900 to 1979, it is the longest homogeneous polar motion data set in existence.

The polar motion and the SOI time series are not, as yet, directly comparable for the following reasons. (i) The polar motion is in fact the temporal convolution of the excitation

function  $\psi$  with the free Chandler wobble, and (ii) the excitation function  $\psi$  of the polar motion contains components that are absent in the SOI and are of no interest as far as ENSO is concerned. These components include a mean value, a linear trend, and a strong annual term. Therefore, I first remove these components from both x- and y-series of the ILS polar motion using linear least-squares. Then I pass the resultant through a Backus-Gilbert deconvolution filter devised by Gross & Chao (1985), using a trade-off coefficient of 1.0. The end result is the observed excitation function  $\psi$  of the Chandler wobble, with x- and y-components,  $\psi_x$  and  $\psi_y$ , as shown in Figures 1(a) and 1(b), respectively. Note that as long as the Chandler band remains our sole interest, it does not matter what type of deconvolution scheme is actually used. Any "raw" deconvolution, such as employed by Wilson & Haubrich (1976) or Wahr (1983), will yield the same coherence in the Chandler band. The main reason we use Backus-Gilbert deconvolution is that it greatly suppresses high-frequency noise in  $\psi$  and hence allows: (i)  $\psi$  to be at all presentable (Figure 1), and (ii) time-domain comparison to be possible (but see Section 4).



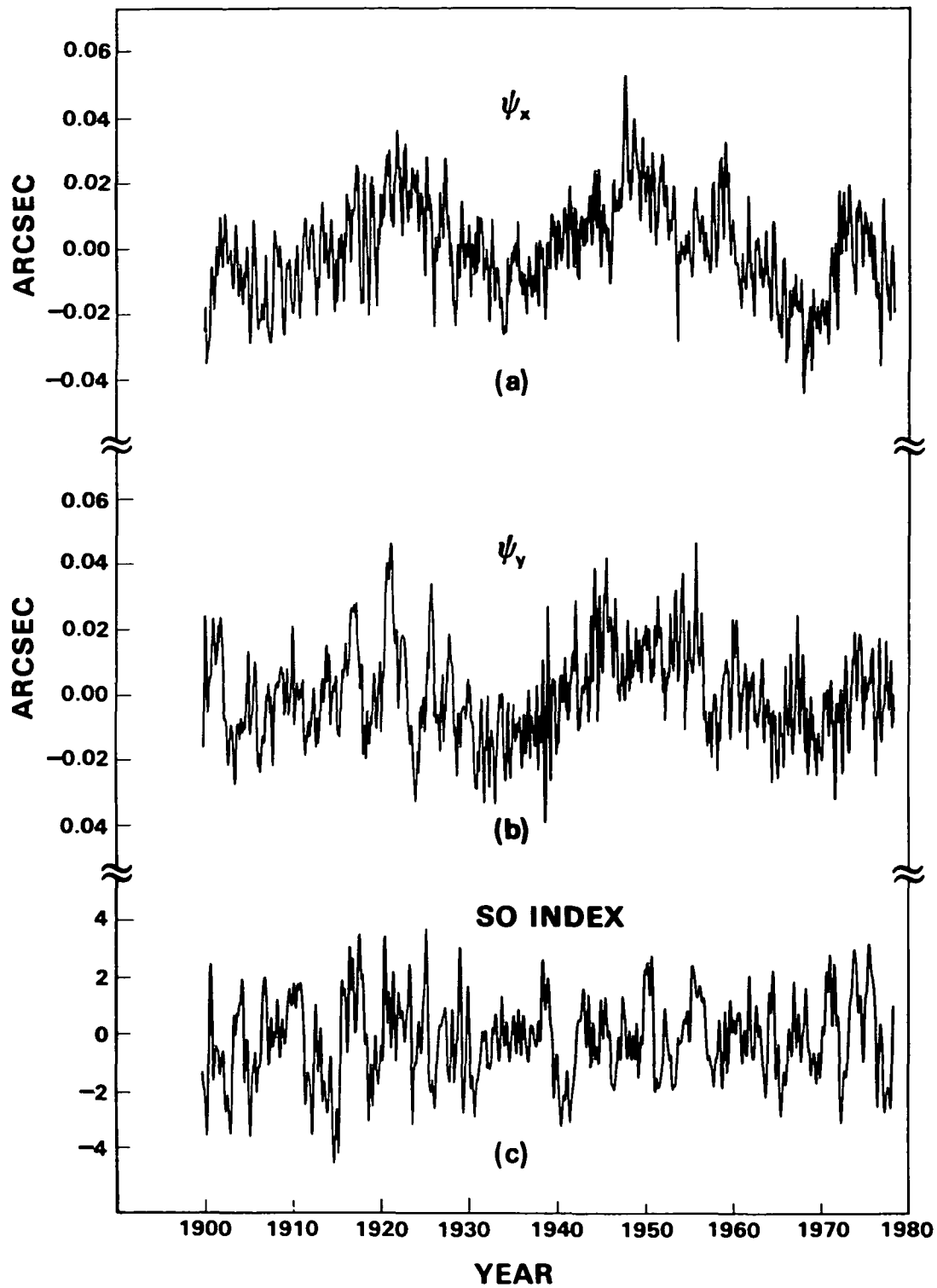


Figure 1. (a) The x-component, and (b) the y-component of the Chandler wobble excitation function derived from ILS data. (c) The southern oscillation index (SOI), 1900-1979.

### 3. COHERENCE STUDY AND RESULTS

The thesis of the present study is to search for linear correlation (in the form of coherence) between the x- and y-components (or "equatorial" components) of the (interannual) angular momentum (call them  $M_x$  and  $M_y$ , respectively) carried by ENSO on the one hand, and the excitation function  $\psi$  of the observed Chandler wobble on the other. In lack of observations for  $M_x$  and  $M_y$ , I am actually using SOI as a proxy, with the hope that it represents  $M_x$  and  $M_y$  in a linear fashion:

$$\begin{aligned} \text{SOI} &= L_x (M_x) \\ \text{SOI} &= L_y (M_y) \end{aligned} \tag{2}$$

where  $L_x$  and  $L_y$  are some linear operators. Equation (2) is a crucial assumption and will be discussed further in Section 4.

Before delving into numerical computations, I shall discuss qualitatively some facts that may be favorable for ENSO to be of importance in the excitation of Chandler wobble. First of all, unlike other geophysical events (such as earthquakes, core-mantle interactions, or solar wind bombardment), ENSO appears to carry sufficient angular momentum to excite Chandler wobble to an observable level. This is argued to be so by Gross & Chao (1985) in an order-of-magnitude assessment. Note, incidentally, that here the angular momentum includes contributions from both velocity and mass redistribution of air masses (see, e.g., Gross & Chao, 1985, Equation 4.4). Secondly, Wilson & Haubrich (1976) and Wahr (1983) have concluded that the atmospheric variation may account for a significant fraction (about 20%) of the total Chandler wobble excitation. Since it is actually the atmospheric energy in the Chandler band (rather than the dominant seasonal energy) which is ultimately responsible, we should look for atmospheric excitation mechanisms of interannual time scale, among which ENSO is undoubtedly a strongest candidate. In fact, a typical El Nino event has a life span of about 14 to 16 months (Wyrтки, 1982). The whole situation is highlighted by the Fourier power spectrum of the SOI time series (Figure 2), which shows a prominent spectral peak at around 447 days, straddling the Chandler band.

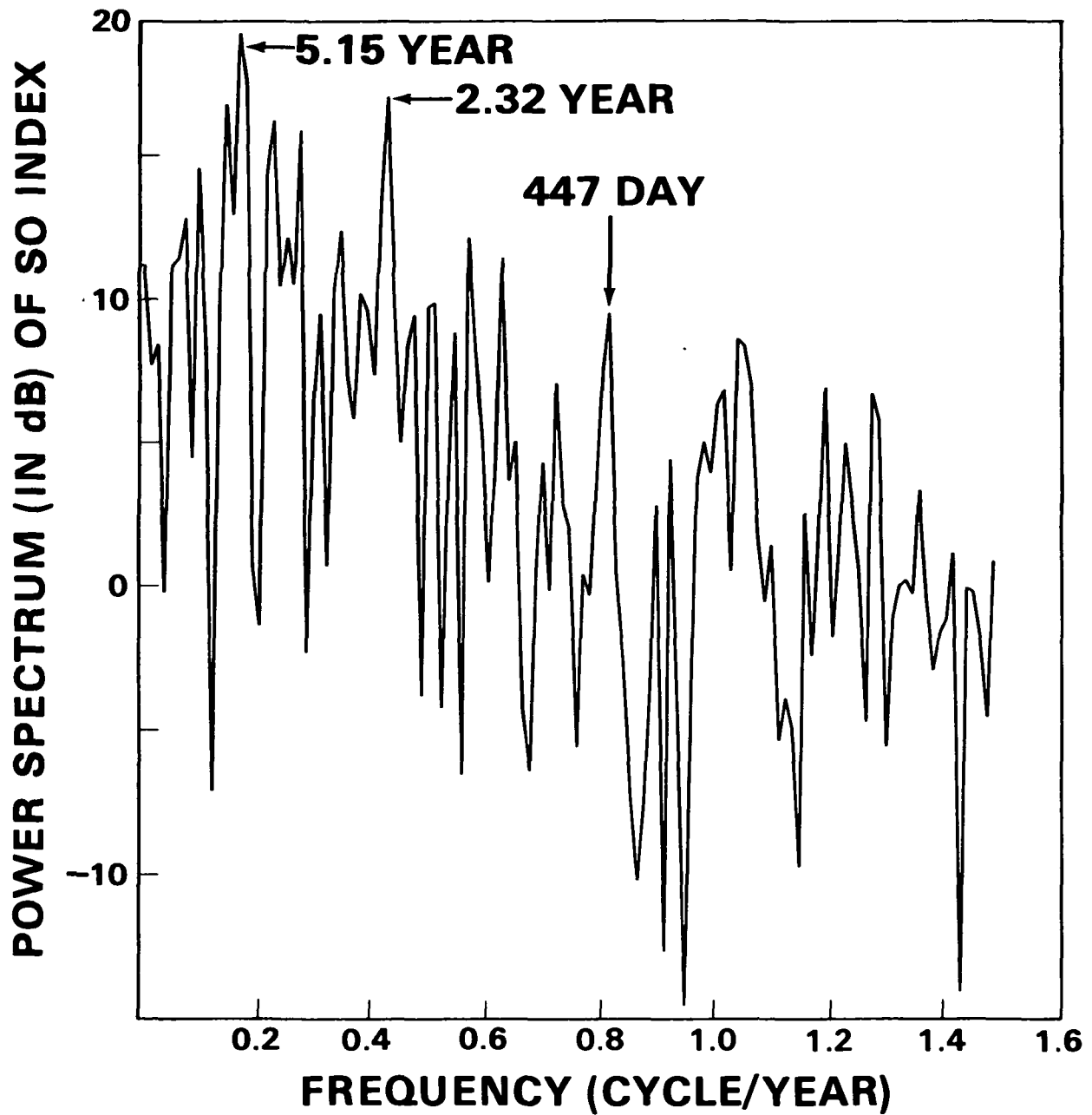


Figure 2. The Fourier power spectrum of the southern oscillation index, SOI (1900-1979). Note the peak (at  $\sim 447$  days) straddling the Chandler band.

The coherence spectrum of two random signals  $x_1(t)$  and  $x_2(t)$  is here defined as

$$\gamma_{12}(f) = \frac{G_{12}(f)}{\sqrt{G_{11}(f) G_{22}(f)}} \quad (3)$$

where  $f$  is frequency,  $G_{12}(f)$  is the (complex-valued) cross-power spectrum of  $x_1(t)$  and  $x_2(t)$ ,  $G_{11}(f)$  and  $G_{22}(f)$  are the (real-valued) auto-power spectra of  $x_1(t)$  and  $x_2(t)$ , respectively.  $\gamma_{12}(f)$ , as defined, is a complex-valued function of frequency and can be expressed as  $|\gamma_{12}(f)| \exp[i\Gamma_{12}(f)]$ , where  $|\gamma_{12}(f)|$  and  $\Gamma_{12}(f)$  are called, respectively, the coherence magnitude and the coherence phase. Because we are usually more interested in high coherence magnitudes, it is convenient (and customary) to display the square of  $|\gamma_{12}(f)|$ , or the coherence power, rather than  $|\gamma_{12}(f)|$  itself. The coherence phase  $\Gamma_{12}(f)$  gives the phase difference between  $x_1(t)$  and  $x_2(t)$  as a function of frequency; and the coherence power  $|\gamma_{12}(f)|^2$  is a normalized measure of correlation between  $x_1(t)$  and  $x_2(t)$ —its value, ranging from 0 to 1, indicates the squared correlation coefficient between  $x_1(t)$  and  $x_2(t)$  at any given frequency.

The power spectra are usually estimated by the discrete Fourier transform (DFT) in the following way:  $\hat{G}_{12}(f) = X_1(f) X_2(f)^*$ ,  $\hat{G}_{11}(f) = |X_1(f)|^2$ ,  $\hat{G}_{22}(f) = |X_2(f)|^2$ , where  $X_1$  and  $X_2$  are the DFT of  $x_1$  and  $x_2$ , respectively. However, DFT being an unstable spectral estimate, this practice results, according to definition (3), in a value of 1 for  $|\gamma_{12}(f)|$  regardless of its true value. In order to produce a more accurate (and hence useful) estimate for  $\gamma_{12}(f)$ , it is necessary to do spectral averaging. A common practice in the present situation is a moving average of the DFT power spectrum estimates:

$$G(f_1) = \frac{1}{N} \sum_{j=-n}^n \hat{G}(f_1 + j) \quad (4)$$

where  $N = 2n + 1$  is the averaging window length. Note that procedure (4) reduces the frequency resolution by a factor of  $N$ . Thus, the spectral averaging stabilizes the estimate for the coherence  $\gamma_{12}(f)$  at the expense of frequency resolution; and the choice of  $N$  should represent a reasonable compromise. Following Bloomfield (1976), the coherence power threshold at, say, 95% confidence level after  $N$ -point spectral averaging is

$$\alpha^2(N) = 1 - 20^{-\frac{1}{N-1}} \quad (5)$$

Only observed value of  $|\gamma_{12}(f)|^2$  greater than  $\alpha^2$  can be regarded as significantly different from 0. For these values, the 95% confidence interval for  $|\gamma_{12}(f)|$  is given approximately by  $(\tanh z_1, \tanh z_2)$  where  $z_1$  and  $z_2$  are

$$\frac{1}{2} \ln \frac{1 + |\gamma_{12}(f)|}{1 - |\gamma_{12}(f)|} \pm \frac{1.96}{\sqrt{2N}}, \quad (6)$$

and the 95% confidence interval for the phase  $\Gamma_{12}(f)$  is approximately (Bloomfield, 1976)

$$\Gamma_{12}(f) \pm \frac{1.96}{\sqrt{2N}} \sqrt{\frac{1}{|\gamma_{12}(f)|^2} - 1} \quad (7)$$

For our 80-year long time series under study, I choose  $N = 7$ . This yields a frequency resolution of 7/80 cpy, somewhat higher than the bandwidth of the Chandler band we defined earlier (and hence is desirable). Equation (5) then, gives  $\alpha^2(7) = 0.39$  as the threshold at 95% confidence level.

Figure 3 shows the computed power  $|\gamma_{12}(f)|^2$  for the pair (SOI,  $\psi_x$ ) and the pair (SOI,  $\psi_y$ ), up to the Nyquist frequency of 6 cpy. The Chandler frequency is indicated by the vertical dashed line and the 95% threshold by the horizontal dashed line. The low-frequency portion, 0-1.5 cpy, of Figure 3 are reproduced in Figures 4(a) and 5(a). Figures 4(b) and 5(b) show the corresponding coherence phase spectra. The most striking feature is the peak near the Chandler frequency in  $|\gamma_{12}(f)|^2$  spectrum for (SOI,  $\psi_x$ ) (Figure 4a). Although its maximum lies some 0.04 cpy off the Chandler frequency, it peaks through the 95% threshold decisively and has most of its energy in the Chandler band. This strongly suggests a considerable correlation between SOI and  $\psi_x$ .

The assertion that SOI and  $\psi_x$  are correlated in the Chandler band is further supported

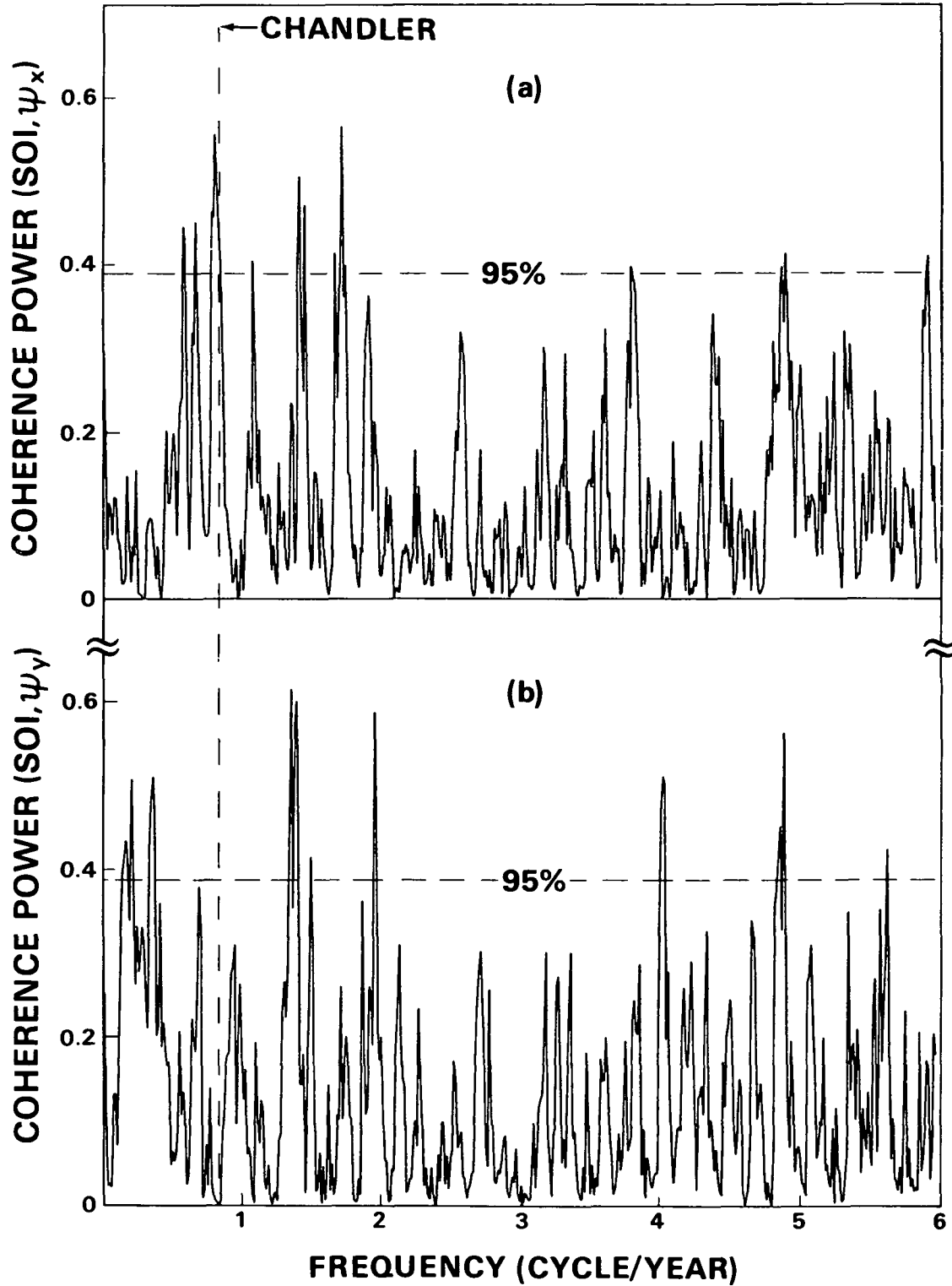


Figure 3. The coherence power for the pair (a) (SOI,  $\psi_x$ ), and (b) (SOI,  $\psi_y$ ), up to the Nyquist frequency. The Chandler frequency and the 95% confidence threshold are indicated by dashed lines

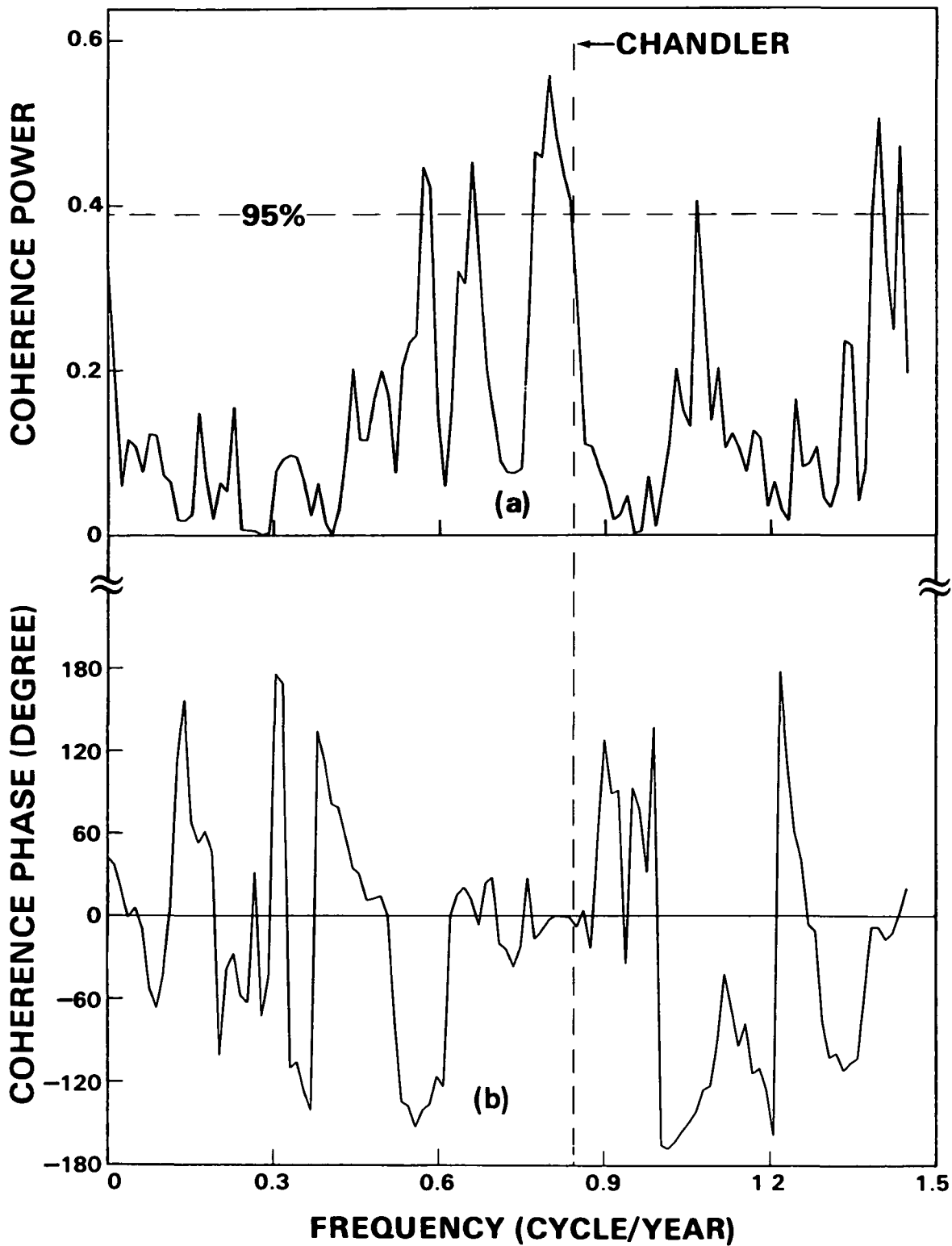


Figure 4. (a) The coherence power, and (b) the coherence phase for the pair (SOI,  $\psi_x$ ), 0-1.5 cpy.

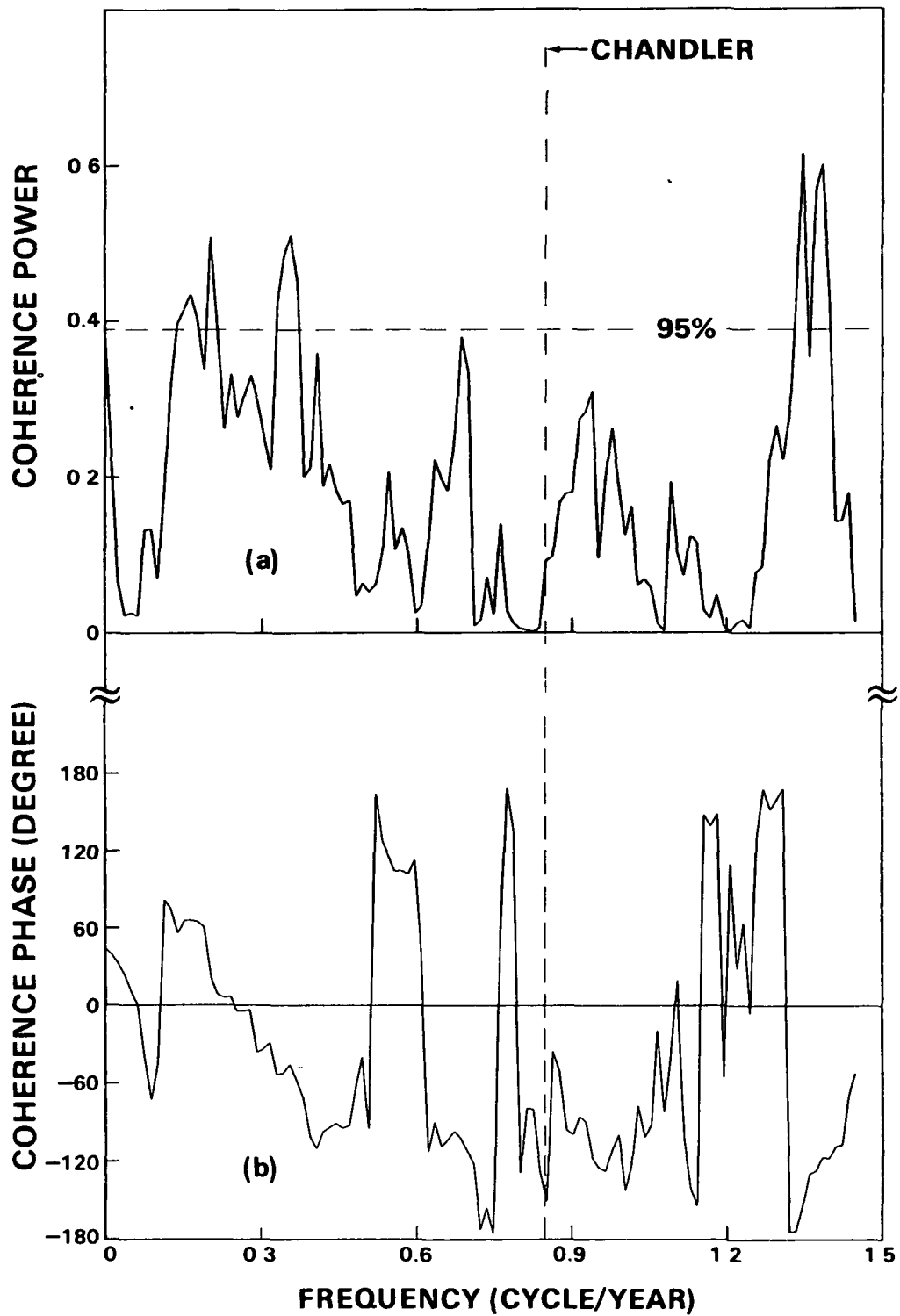


Figure 5. (a) The coherence power, and (b) the coherence phase for the pair (SOI,  $\psi_y$ ), 0-1.5 cpy.



by their coherence phase spectrum (Figure 4b). Theoretically, a necessary condition of this assertion is that the phase be fairly constant in the Chandler band. In the present case, we should expect SOI and  $\psi_x$  to be in phase, or, their phase difference in the Chandler band to be zero. This is exactly what Figure 4(b) shows. The fact that maximum coherence power coincides with zero coherence phase boosts our confidence in the relationship well over the 95% level.

Using Equations (6) and (7), we can now put statistical bounds on the coherence estimates in the Chandler band. Since these bounds are themselves functions of the magnitude  $|\gamma_{12}(f)|$ , let us simply choose a representative estimated value for  $|\gamma_{12}(f)|$  in the Chandler band:  $|\gamma_{12}(f)| = \sqrt{0.45} = 0.67$  (see Figure 4a). Then, the 95% confidence interval for  $|\gamma_{12}(f)|$  is found to be (0.28, 0.87), and the 95% confidence interval for the phase  $\Gamma_{12}(f)$  to be  $0^\circ \pm 33^\circ$ . The implication of these values will be discussed in the next section.

Interestingly enough, the situation with (SOI,  $\psi_y$ ) is quite the opposite—the coherence power between SOI and  $\psi_y$  reaches a minimum and approaches zero in the Chandler band (Figure 5a). The lack of correlation is further evidenced by an erratic fluctuation of the coherence phase in the Chandler band (Figure 5b).

#### 4. DISCUSSION AND CONCLUSION

The ILS data are known to contain serious systematic as well as random errors. That is the reason why a time-domain study of the correlation between SOI and  $\psi$  (which I also conducted) proved to be unfruitful—the overall (temporal) correlation coefficients found [ $\sim 0.10$  for  $(\text{SOI}, \psi_x)$  and  $\sim 0.15$  for  $(\text{SOI}, \psi_y)$ ] fall well below the level of significance. I have also compared SOI with both  $\psi_x$  and  $\psi_y$  in the time domain (c.f. Figure 1) for each individual El Nino period; these comparisons, ranging from “remarkable” to “awful”, show no consistent pattern whatsoever. Indeed, it is when we enter the frequency domain that we see something meaningful. This is because the Fourier transformation concentrates a periodic signal (the Chandler wobble in this case) into a narrow frequency band (the Chandler band), while it spreads the noise over the whole spectrum. A corollary of this statement is that the ILS signal in the Chandler band (as well as the annual band in which we are not interested) has a signal-to-noise ratio of as high as 20-30 dB whereas any other frequency contains practically nothing but noise. Therefore, for example, we should ignore the coherence outside the Chandler band even if its power exceeds the 95% threshold (see Figure 3). At any rate, since we are here only interested in the Chandler band it is fair to say that the noise in the ILS data does not pose a serious problem to the present study.

A more serious problem (in a philosophical sense at least) is associated with the linearity assumption (2), the need for which, as stated earlier, arises because the coherence study only looks for linear relationships. There are indications that SOI is essentially linearly related to the z- (or “axial”) component of the atmospheric angular momentum carried by ENSO (see Chao, 1984, Figure 4). But there has been no telling of its validity with respect to the x- and y-components. Any nonlinearity can result in biases in the coherence spectra. This might explain the (unexpected) total lack of coherence between SOI and  $\psi_y$  and the fact that the coherence maximum for  $(\text{SOI}, \psi_x)$  lies somewhat off the Chandler frequency. In any event, the a postereori finding that  $(\text{SOI}, \psi_x)$  coherence shows zero phase offset and large magnitude in the Chandler band does suggest linearity to a large extent.

So far we have ignored the  $\sim 30$ -year oscillation in the ILS data, which can be clearly seen in Figures 1(a) and 1(b). This oscillation is known as the Markowitz wobble although its origin is largely unknown (see Dickman, 1983). The presence of Markowitz wobble does not affect our results, however, because its associated energy is concentrated in the extreme low-frequency end of the spectrum. This is confirmed by a numerical experiment which shows that the differences in coherence spectra resulting from the removal of the Markowitz wobble are strictly confined to frequencies lower than 0.05 cpy. Furthermore, since at these low frequencies the coherence between SOI and  $\psi$  (with or without Markowitz wobble) is not significant, we conclude that Markowitz wobble is not linearly correlated with ENSO.

The conclusion of this study, thus, is that ENSO is correlated with the excitation of the Chandler wobble to a significant degree during 1900-1979 in the following sense. The correlation seems to be all concentrated in the pair (SOI,  $\psi_x$ ); that between SOI and  $\psi_y$  is practically nil. The correlation between SOI and  $\psi_x$  is in the neighborhood of 0.67, with the 95% confidence interval of  $\sim (0.28, 0.87)$  (see Section 3). Since physically ENSO and Chandler wobble are involved here in a cause-and-effect relationship (ENSO being the "input" and Chandler wobble being the "output" of the Earth filter), this, in terms of power, means that ENSO accounts for 45% of the x-component of the excitation power for the Chandler wobble, or, since the excitation powers for x- and y-components are nearly the same (c.f. Figure 1), some 20% of the total excitation power. Although the associated 95% confidence interval, (4%, 38%), is not as severe a constraint as we like it to be, 20% agrees well with the amount of Chandler wobble excitation due to the entire atmosphere/ocean system determined by Wahr (1983). The implication here is that ENSO is indeed an important (interannual) part of the atmospheric/oceanic variation that is responsible for the excitation of Chandler wobble during 1900-1979. Note that the finding here is a far cry from the pessimistic view I held in an earlier, preliminary report on this study (Chao, 1984). The latter came about primarily because in computing the coherence phase spectra I had adopted Wilson & Haubrich's (1976) algorithm which does with-

out spectral averaging. That yielded extremely unstable raw estimates which, in turn, completely obscured the true coherence and made the interpretation difficult.

One final note deserves discussion. Using accurate LAGEOS polar motion data, Gross & Chao (1985) claim that the strong 1982-1983 ENSO episode has left its signature in the y-component  $\psi_y$  of the excitation function of Chandler wobble, but not in the x-component  $\psi_x$ . This is opposite to what 1900-1979 data show in this study, and seems surprising at first. However, if we take a close look at the anomalous behavior of the 1982-1983 ENSO event, this x-y reverse situation may not be surprising after all. It is well-known (see, e.g., Rasmusson & Wallace, 1983) that the 1982-1983 ENSO event, apart from being the strongest on record, has an unusual timing relative to the climatological annual cycle—it was delayed by about half a year compared with usual ENSO events. Spatially, it also appears that the 1982-1983 weakening of SO was due to high air pressure at Darwin and the pattern of warm water moving eastward, in contrast to a typical ENSO episode where the SO weakening is caused by low air pressure at Tahiti and the warm water pattern moving westward. Clearly these differences in behavior are immaterial as far as the effect on the z-component of the atmospheric angular momentum (and hence on the length-of-day) is concerned. However, their effect on the x- and y-components of the atmospheric angular momentum (and hence on Chandler wobble) is a much subtler problem. The said half-cycle offset in the timing and the reversal in the spatial pattern may provide the explanation for the above observed x-y reverse situation. It is worthwhile to note that, if this is the case, the Earth's polar motion is providing us with a clear gross indication on a meteorological variable. The previous known ENSO event that has a similar unusual timing is that of 1940-1941, which, interestingly enough, is probably the strongest event on record before the 1982-1983 event (Rasmusson & Wallace, 1983) (but obviously one single event cannot produce any significant coherence to be observed in the spectrum). The time-domain comparison between SOI and  $\psi$  time series (mentioned above) for the period 1940-1941 does show a better comparison for (SOI,  $\psi_y$ ) than for (SOI,  $\psi_x$ ). Furthermore, during 1940-

1941, like in 1982-1983 (see Gross & Chao, 1985),  $\psi_x$  was relatively quiescent (c.f. Figure 1). But these should not be considered conclusive because, again, the noise in ILS data is too high to render any detailed time-domain comparison meaningful. If the above argument is valid then, in light of the findings in Gross & Chao (1985) and in this study, it seems that the conventional geographical coordinate system (which is purely artificial) coincides (luckily) with an "optimum" designation of the x and y axes as far as the ENSO effect is concerned. The reason may lie in the fact that the southern oscillation is largely anti-symmetric with respect to the dateline (in the negative x direction) although the ENSO effect is felt globally.

#### ACKNOWLEDGMENTS

I am grateful to R. S. Gross for his help in the processing of the polar motion data and to T. M. Eubanks for discussions.

## REFERENCES

- Bloomfield, P., *Fourier Analysis of Time Series: An Introduction*, John Wiley & Sons, New York, 1976.
- Chao, B. F., The excitation of Chandler wobble by the southern oscillation based on ILS data, *EOS Trans. AGU*, 65, 859, 1984.
- Dickman, S. R., The rotation of the ocean-solid Earth system, *J. Geophys. Res.*, 88, 6373-6394, 1983.
- Eubanks, T. M., J. O. Dickey, and J. A. Steppe, The 1982-83 El Nino, the southern oscillation, and the length of day, *Tropical Ocean and Atmosphere Newsletter*, in press, 1985.
- Gross, R. S., and B. F. Chao, Excitation study of the LAGEOS derived Chandler wobble, *J. Geophys. Res.*, in press, 1985.
- Munk, W., and E. S. M. Hassan, Atmospheric excitation of the Earth's wobble, *Geophys. J. Roy. Astron. Soc.*, 4, 339-358, 1961.
- Quinn, W. H., D. O. Zopf, K. S. Short, and R. T. W. Kuo Yang, Historical trends and statistics of the southern oscillation, El Niño, and Indonesian droughts, *Fish. Bull.* 76, 663-678, 1978.
- Rosen, R. D., D. A. Salstein, T. M. Eubanks, J. O. Dickey, and J. A. Steppe, An El Nino signal in atmospheric angular momentum and Earth rotation, *Science*, 225, 411-414, 1984.
- Rasmusson, E. M., and J. M. Wallace, Meteorological aspects of the El Nino/southern oscillation, *Science*, 222, 1195-1202, 1983.
- Wahr, J. M., The effects of the atmosphere and oceans on the Earth's wobble and on the seasonal variations in the length of day—II. Results, *Geophys. J. Roy. Astron. Soc.*, 74, 451-487, 1983.
- Wilson, C. R., and R. A. Haubrich, Meteorological excitation of the Earth's wobble, *Geophys. J. Roy. Astron. Soc.*, 46, 707-743, 1976.
- Wyrtki, K., The southern oscillation, ocean-atmosphere interaction and El Nino, *Mar. Tech. Soc. J.*, 16, 3-10, 1982.

**Yumi, S., and K. Yokoyama, Results of the International Latitude Service in a homogeneous system (1899.9-1979.0), Central Bureau of the International Polar Motion Service, Mizusawa, Japan, 1980.**

## BIBLIOGRAPHIC DATA SHEET

1. Report No. NASA TM-86231	2. Government Accession No.	3. Recipient's Catalog No.	
4. Title and Subtitle <b>EXCITATION OF THE EARTH'S CHANDLER WOBBLE BY SOUTHERN OSCILLATION / EL NINO, 1900- 1979</b>		5. Report Date September 1985	
		6. Performing Organization Code 621	
7. Author(s) B. Fong Chao		8. Performing Organization Report No. 85BO557	
9. Performing Organization Name and Address Geodynamics Branch Laboratory for Terrestrial Physics GSFC. Greenbelt, Maryland 20771		10. Work Unit No.	
		11. Contract or Grant No.	
		13. Type of Report and Period Covered  Technical Memorandum	
12. Sponsoring Agency Name and Address  NASA Washington, D.C. 20546		14. Sponsoring Agency Code	
15. Supplementary Notes			
16. Abstract  The southern oscillation / El Nino (ENSO) is the single most prominent interannual signal in global atmospheric/oceanic fluctuations. This paper addresses the following question: how important is the angular momentum carried by ENSO in exciting the Earth's Chandler Wobble? The question is attacked through a statistical analysis of the coherence spectra (correlation as a function of frequency) between two data sets spanning 1900-1979—the southern oscillation index (SOI) time series and the excitation function $\psi$ (with x-component $\psi_x$ and y-component $\psi_y$ ) of the Chandler wobble derived from the homogeneous ILS (International Latitude Service) polar motion data. The coherence power and phase in the Chandler frequency band ( $\sim 0.79$ - $0.89$ cpy) are studied. It is found that, during 1900-1979 the coherence between SOI and $\psi_x$ is significant well over the 95% confidence threshold whereas that between SOI and $\psi_y$ is practically nil. Quantitatively, the coherence study shows that ENSO provides some 20% of the observed Chandler wobble excitation power. Since earlier investigations have shown that the total atmospheric/oceanic variation can account for the Chandler wobble excitation at about 20% level, the implication is that ENSO may be an important (interannual) part of the atmospheric/oceanic variation that is responsible for the Chandler wobble excitation during 1900-1979.			
17. Key Words (Selected by Author(s))  Chandler Wobble Excitation ENSO		18. Distribution Statement  Category Listing	
19. Security Classif. (of this report)  Unclassified	20. Security Classif. (of this page)  Unclassified	21. No. of Pages	22. Price*